Medium Scale CBR Anisotropy Measurements: UCSB South Pole HEMT (1990-91) and MAX 3 (1991)

Peter Meinhold[1,2] *with the ACME-HEMT and MAX Collaborations*

[1] The University of California at Santa Barbara
[2] The NSF Center for Particle Astrophysics

1 Introduction

The COBE detection of anisotropy in the Cosmic Background Radiation has spurred interest in comparisons between large, 'medium' and small angular scales. Since the COBE announcement, most calculations have used theoretical scenarios of Galaxy formation, along with a normalization of the primordial perturbation spectrum derived from the COBE data, to predict fluctuations at angular scales of 0.5- several degrees. A number of experiments have been done at these angular scales, with interesting results. CBR anisotropy results from the UCSB South Pole expedition (1990-1991), and the third flight of the Millimeter Anisotropy Experiment (MAX) experiment (1991) are presented. These two experiments probe the angular range from roughly 10 arcminutes to 3 degrees, crucial for testing theories of structure formation.

Our HEMT measurements made from the South Pole over a range of frequency from 25 to 35 GHz, with a beamsize of 1.5 degrees, have been used to set stringent constraints on structure formation theories normalized by the COBE detection. For a Gaussian Autocorrelation Function (GACF) model, these data provide an upper limit of 1.5×10^{-5} at 1.2 degrees. Structure is observed in the data at a level of $\Delta T/T \approx 8 \times 10^{-6}$, with spectrum consistent with that expected from CBR fluctuations, but more consistent with Galactic foreground contamination.

Balloon borne bolometric measurements by the MAX experiment in the frequency range from 180 to 360 GHz have detected interstellar dust, as well as significant structure possibly due to CBR fluctuations. Two separate regions of sky were measured, and after subtraction of an interstellar dust (ISD) component, the data from one region have been used to derive a new upper limit for a GACF of $\Delta T/T < 2.5 \times 10^{-5}$ at 25 arcminutes. The second region (with no ISD removal needed) shows a highly significant detection of structure, with a spectrum consistent with CBR anisotropy. The observed structure corresponds to a GACF amplitude of $\Delta T/T = 4.2^{+1.7}_{-1.1} \times 10^{-5}$, for a coherence angle of 25 arcminutes.

It should be explicitly stated here that the GACF upper limits are only quoted in order to allow a relatively experiment independent way to compare

results. GACF limits at a given angular scale can be compared with each other, and can be used to test the (common) assumption of Gaussian *distributed* fluctuations as opposed to fluctuations well approximated by a GACF.

2 Foreground Contamination

Experiments attempting to measure CBR anisotropy at the level of a few parts in 10^6 are prone to systematic errors associated with four principal foregrounds: Emission from the Earth's atmosphere, off-axis (sidelobe) pickup of emission from the Earth, Moon, Sun, or other objects, diffuse emission from the interstellar medium (warm dust or radiation from charged particles), and extragalactic radio sources.

2.1 Atmosphere

The two experiments described here, ACME-HEMT 1990-1991, and the MAX experiment, rely on a choice of site and operating frequencies to reduce atmospheric emission. The ACME-HEMT system is a coherent amplifier system, and uses relatively narrow passbands (4 bands covering a total of 10 GHz centered at 30 GHz) in a frequency region with low atmospheric emission, operating from a high dry site (the South Pole). MAX is a bolometric system, operating over a much broader frequency span (3 bands at roughly 20-30 % bandwidth centered near 180, 270 and 360 GHz), and thus receives emission from many more atmospheric lines. MAX consequently observes from an altitude of 35 km to reduce the atmospheric signal.

2.2 Sidelobe Contamination

Both experiments use a Gregorian telescope with 1 meter focal length, underfilling both the elliptical secondary and the primary mirrors. The primary mirror and associated telescope mount and pointing system are common to the two experiments, although configured differently for ground and balloon operation. The underfilled optics and lack of obstruction in the primary beam afford very low sidelobe response for each system. Large reflective baffles are used to further reduce the effects of far sidelobe response. The telescope response has been mapped in one dimension to a level of more than 65 dB below the on-axis response for both ACME-HEMT and MAX. Measurements made during the third flight of MAX imply no significant contamination from sidelobe response. Data taken closer than 65 degrees from the Sun during the ACME-HEMT South Pole 1990-1991 expedition are possibly contaminated by solar emission at the part in 10^5 level, and consequently these data are rejected.

2.3 Galactic Foregrounds

Figure 1 shows the spectral characteristics of the expected Galactic foregrounds, in addition to that of a CBR anisotropy. The bandpasses of the two instruments

are sketched in to illustrate the spectral discrimination used in the experiments. The absolute levels of the three Galactic foregrounds have been arbitrarily chosen, but are consistent with the levels expected for reasonably good regions away from the Galactic plane. Note that ACME-HEMT is best able to distinguish between synchrotron and bremsstrahlung radiation and CBR anisotropy, while MAX is extremely good at distinguishing ISD emission from CBR.

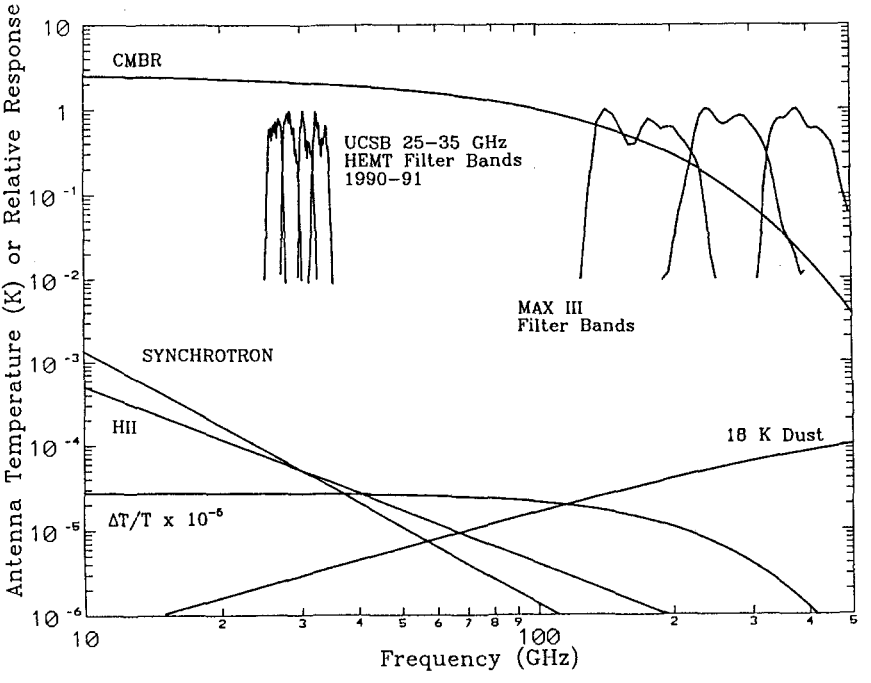

Fig. 1. Spectral characteristics of Galactic foregrounds far from the Galactic plane, presented in terms of antenna temperature. Power received in a single mode HEMT system is proportional to T_A, while that received by a constant throughput system like MAX is proportional to $\nu^2 T_A$. Free-free and Synchrotron specific intensity are set equal to 50 μK at 30 GHz, assumed to scale as $S(\nu) \propto \nu^{-2.1}$ and $S(\nu) \propto \nu^{-2.7}$ respectively. Dust emission assumes 18.5 K dust with emissivity $\propto \nu^{1.4}$

2.4 Extragalactic Sources

Flat spectrum extragalactic radio sources pose similar problems for ACME-HEMT and for MAX. Many types of spectra have been observed from different objects, making discrimination of CBR fluctuations from spectral information alone problematic. The general technique is to use low frequency surveys at high resolution, and morphological considerations to identify possible extragalactic contaminating sources. Potentially contaminated regions can then be mapped using ground based high resolution telescopes at several frequencies.

3 ACME-HEMT South Pole, 1990-1991

ACME-HEMT 1990-1991 refers to an expedition made to the South Pole from November, 1990 to January, 1991 to measure CBR anisotropy using the ACME telescope equipped with an extremely low noise, liquid ^{4}He cooled, direct amplification High Electron Mobility Transistor (HEMT) receiver (Pospieszalski et al, 1990). The telescope produced a 1.5 degree full width at half maximum (FWHM) response at 30 GHz, moved sinusoidally on the sky with peak to peak separation of 2.1 degrees. The beamsize varies as FWHM $\propto \nu^{-1}$. Data from this expedition have recently been published in Gaier et al (1992), and Schuster et al (1993).

3.1 Detector

The detector consisted of a HEMT amplifier cooled to 4.2 K with liquid Helium, with a noise temperature of 30 K, and a 10 GHz bandpass centered around 30 GHz. This was followed by a warm amplifier and a set of circulators and filters designed to produce 4 channels of 2.5 GHz each. In the absence of atmospheric noise, the expected sensitivity was 1.4mK$\sqrt{\text{sec}}$ in terms of $\Delta T/T$ for each channel. The actual measured noise (during good weather) varied from 1.8 to 3 mK $\sqrt{\text{sec}}$.

3.2 Measurement Strategy and Raw Data Set

The telescope beam was chopped through 2.1 degrees peak to peak, at 8 Hz. A lockin amplifier demodulated the detector output using a square wave weighting phased with the position of the secondary mirror, providing a first difference measurement of the sky on 0.5 second timescales. The basic measurement strategy consisted of sequentially stepping through a set of points, integrating on each for roughly 20 seconds. The telescope then reversed direction and stepped back through the points. The points were chosen to make the positive lobe from one integration overlay the negative lobe from the adjacent one. This motion over all the points and back is referred to as a full scan. A set of data was obtained including 24 hours worth of 9 point full scans on each of 6 adjacent elevations, as well as deeper integrations on a 13 and a 15 point strip overlaying some of the 9 point strips. The region covered is shown schematically in Figure 2. Measurements of the Moon, the Sun, the Galactic plane, and the Large Magellanic Cloud (LMC) were also performed for pointing and telescope calibration. The detector was calibrated with an ambient load 1 to 2 times per day.

The raw data were edited according to weather, (bad weather were usually identified by a dramatic increase in the noise), calibrations, and chopper instabilities. The data were fit to remove slowly varying offsets and a time varying gradient due to large scale atmospheric structure. The effects of this fitting procedure have been included in the calculations comparing the data to models. The data were then binned in angle and averaged. An error bar was calculated for each bin from the dispersion of the data in the bin, assuming Gaussian noise.

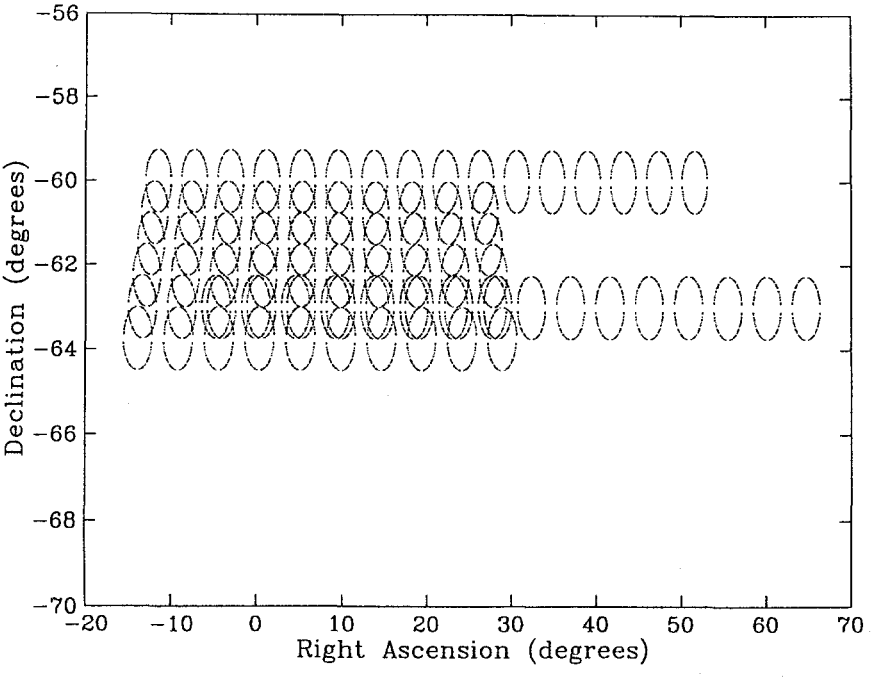

Fig. 2. Orientation of ACME-HEMT 1990-1991 data set. Circles represent half power points of positive or negative lobes of telescope response.

Typical per channel error bars for the best strips are about 22 μK, with a lowest error of 18 μK.

3.3 9 Point Data Set

The 9 point data set with the most integration time has been published in Gaier et al (1992). It consisted of 9 adjacent points centered near $\alpha = 0.5$ hours, $\delta = -62.25°$. This data set is shown in Figure 3. There is a signal in the three lower frequency channels which is essentially absent in the highest frequency channel, suggesting to the eye at least that the signal is not thermal (as CBR would be). The analysis of this data set has been performed a number of different ways by ourselves as well as others. The most probable signal is spectrally inconsistent with CBR anisotropy at the 2 sigma (95 % confidence) level, a result obtained via a number of techniques. The four channels are however *marginally* consistent with a 20 μK rms CBR anisotropy. The effects of the beamsize variation between channels have not been included in the analysis. Inclusion of this variation in the spectral calculation tends to reduce the probability that the measured structure could be CBR anisotropy. Results from our published analysis of this data set, using the highest frequency channel for setting upper limits to CBR anisotropy, are included in Figure 9. For that calculation we have assumed that the signal in the lower frequency channels is due to foreground contamination and that

the highest frequency channel is thus the least contaminated. This upper limit is increased by about 25 % if one assumes a 20 μK rms CBR anisotropy, the amplitude implied by coadding the 4 channels assuming a CBR spectrum.

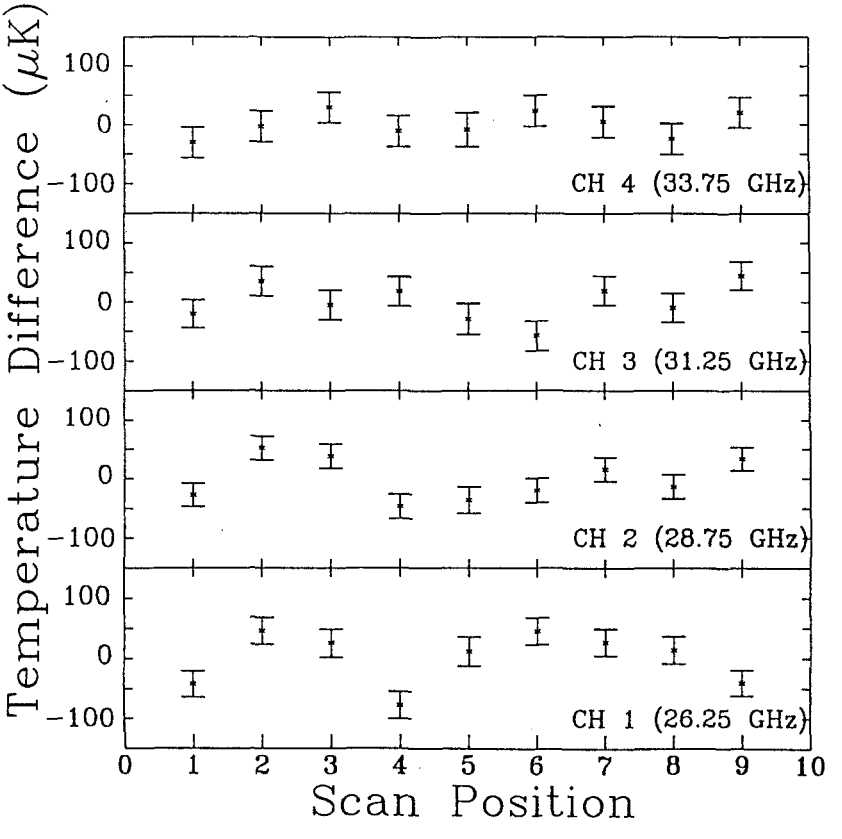

Fig. 3. 9 point data set from $\delta = -62.25°$. Vertical axis is in antenna temperature units, which are the same as thermodynamic temperature units for these frequencies.

3.4 15 Point Data Set

The deepest integration from this expedition was performed on 15 points centered near $\alpha = 2$ hours, $\delta = -63°$. See Schuster et al (1993). A portion of these data were taken with the Sun substantially closer in angle to the measurement region. Some evidence for solar contamination prompted the removal of all data when the Sun was closer than 65 degrees from the measured point. This resulted in only 13 valid data points, which are displayed in Figure 4. These data show a signal, present in all four channels, with substantially higher signal to noise than the signal seen in Figure 3. The spectrum of the most probable signal is

consistent with CBR, but is more consistent with Galactic emission. Figure 5 shows the results of coadding the separate channels, under the assumption that all signal is due to CBR anisotropy (this is not the most probable spectrum, but is useful for conservative upper limit calculations). Note that the error bars on this data set are about 11 μK or $\Delta T/T = 4 \times 10^{-6}$

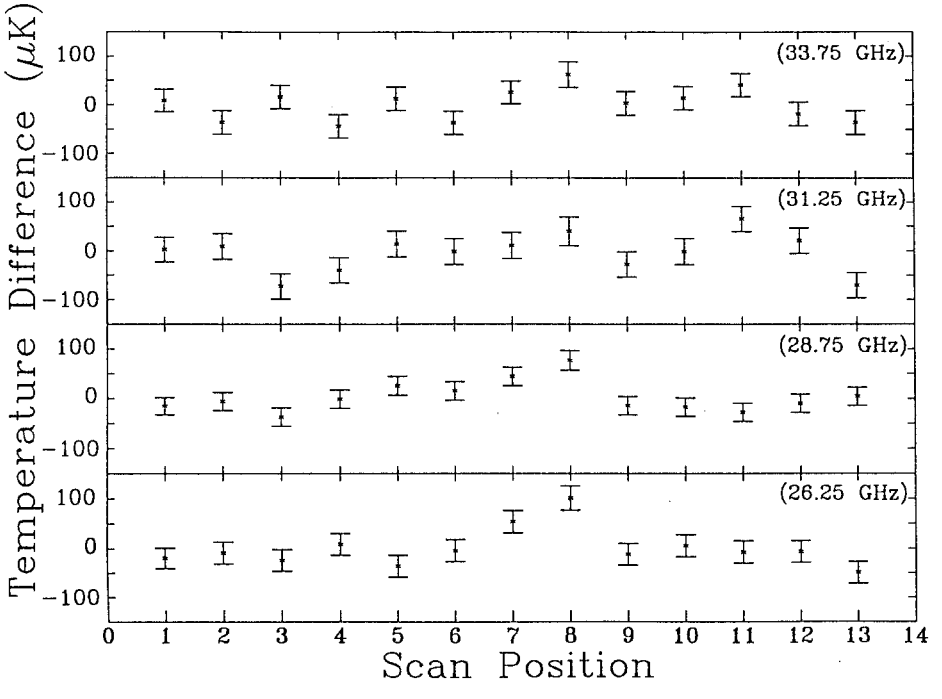

Fig. 4. 13 points of the 15 point data set from $\delta = -63°$.

A conservative analysis for upper limit calculations has been performed, assuming all the signal to be due to CBR anisotropy. Although the per pixel error bars for this data set are smaller than for the data described above, the presence of a signal results in an upper limit of $\Delta T/T < 1.6 \times 10^{-5}$, slightly above those obtained from the 9 point data set. The results are consistent with the 9 point data set, and would imply a CBR anisotropy of $\Delta T/T = 8 \times 10^{-6}$ for a GACF in the most sensitive angular range of 0.75 to 1.5 degrees if all the signal were attributed to the CBR. The upper limit curves from both data sets along with the most probable amplitude curve for the 15 point data set are included in the final plot, Figure 9. The consistency between the two data sets is clear from the figure.

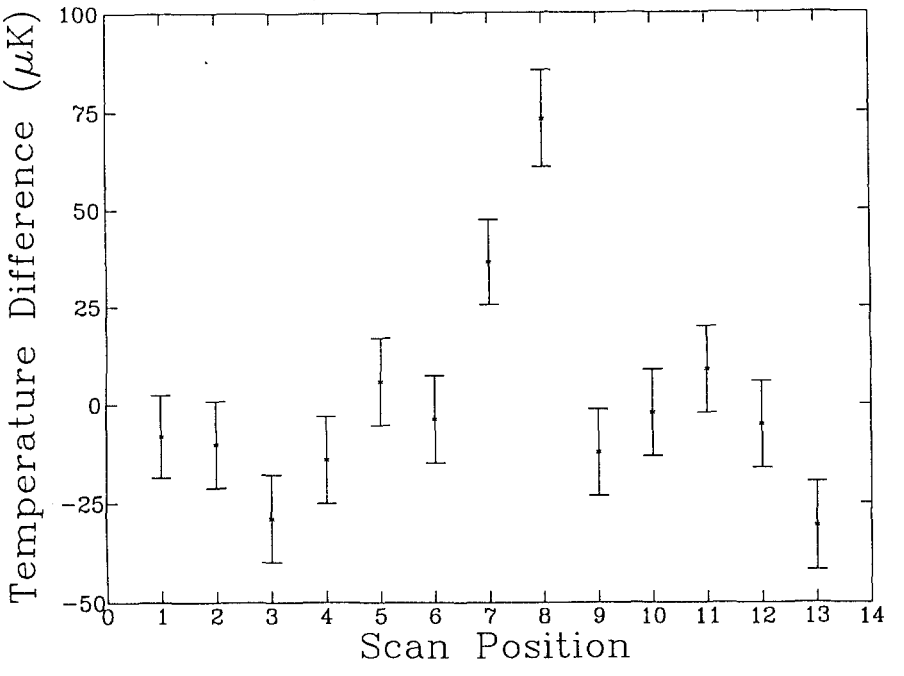

Fig. 5. Coadded data from Figure 4, under the assumption that all signal is due to CBR anisotropy

4 MAX 3

MAX consists of a multi-band dichroic bolometric photometer feeding the 1 meter Gregorian telescope described above. The system produces a FWHM of 0.5 degrees for each band. The elliptical secondary mirror nutates in a sinusoidal fashion to move the beam 1.3 degrees peak to peak on the sky. See Fischer et al (1992) and Meinhold et al (1993a) for more information about the MAX system. The data discussed below (the third flight of MAX) were taken with the system in a configuration using 3 bands, centered near 180, 270, and 360 GHz, with 20 to 30 % bandwidths. The photometer was cooled to 300 mK with a closed cycle ^{3}He refrigerator, and the detectors obtained a sensitivity to CBR fluctuations of 530, 770, and 2764 $\mu K\sqrt{sec}$ respectively.

The third flight of MAX took place on June 6, 1991 from Palestine, Texas. Several hours of high quality data were obtained, including two long integrations to search for fluctuations in the CBR. The data were deglitched to remove occasional cosmic ray and RF interference pulses, demodulated, and then coadded in azimuth angle on the sky. The measured statistical errors were comparable to the detector noise as measured in the laboratory. Calibrations of the system to antenna temperature were performed using a partially reflective membrane

inserted into one lobe of the chopped beam at the focus. Jupiter was used to check this calibration. Data from this flight have been published in Devlin et al (1992), Meinhold et al (1993b), and Gundersen et al (1993).

4.1 Mu Pegasi

The longest integration was carried out around the star Mu Pegasi. The telescope was scanned smoothly $\pm 3°$ back and forth in azimuth for 1.4 hours. This integration occurred when Mu Pegasi was in the east, resulting in little rotation of the measured points relative to the telescope. Figure 6 shows the data from this integration, along with a calculation of the response of the MAX system to ISD emission derived from the high resolution IRAS 100 micron maps. The IRAS data have been scaled vertically for best fit for each band. There is an extremely good correlation between the IRAS data and the MAX measurements, leaving little doubt that most of the measured structure is due to ISD emission. The successful measurement of dust morphology at such a small level (10-50 μK) also demonstrates how far the system noise integrates down, and how well sidelobes and a number of other potential systematic problems have been controlled.

We have performed a variety of fits to the data of Figure 6 to ascertain what constraints they can place on CBR fluctuations. One method assumes two morphologically independent and spectrally distinct components contribute to the data. To constrain CBR fluctuations, we force the spectrum of one component to be that of a CBR anisotropy. These fits produce one component which is morphologically and spectrally like the ISD traced by the IRAS 100 μ maps, and a second component, possibly independent of the dust. This second component is not stable to the details of the data analysis, and is therefore only used as a conservative way of estimating upper limits to CBR anisotropy, by assuming that all the signal in this component is due to the CBR. This assumption leads to an upper limit to CBR fluctuations of $\Delta T/T < 2.35 \times 10^{-5}$ for a GACF at an angular scale of 25 arcminutes (the most sensitive scale). If the residual signal were assumed to be due to CBR anisotropy, it would imply $\Delta T/T = 1.4 \times 10^{-5}$ for a GACF at 25 arcminutes.

4.2 Gamma Ursae Minoris

The second long integration of the MAX 3 flight was carried out around the star Gamma Ursae Minoris (GUM). This region was chosen because a previous flight (Alsop et al, 1992) had shown evidence for structure with a spectrum consistent with CBR anisotropy and inconsistent with ISD emission. In addition, this is a region of sky with low dust emission, with dust contrast (as measured by the IRAS satellite at 100 μ) a factor of 5 below that in the region around Mu Pegasi. This region is located near the North celestial pole, and consequently rotates significantly relative to the local horizon during the measurement. A sample of 16 of the 39 pixels measured is shown in Figure 7. The essential features of the data set are evident in the figure. There is a very significant structure in the data which correlates well between channels, and decreases in amplitude with

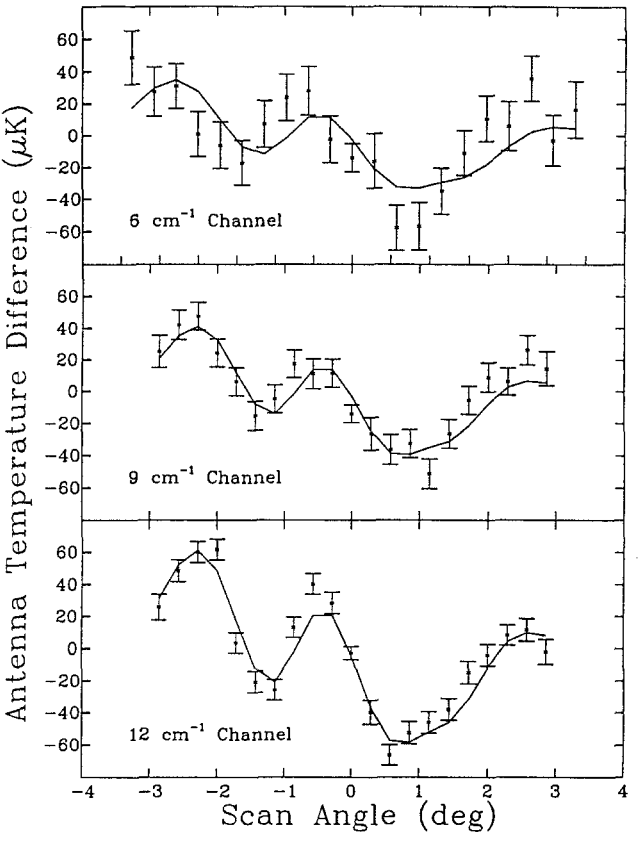

Fig. 6. MAX III data from measurement near the star Mu Pegasi (error bars). A model of dust emission based entirely on the IRAS high resolution 100 micron maps with a scale factor for each MAX channel is shown as solid lines. Note that the vertical axis is in Antenna temperature units: The 6,9, and 12 cm^{-1} channels need to be scaled by 2.3, 5.6, and 22.5 respectively to reference to a 2.7 K blackbody.

increasing frequency, as calibrated in antenna temperature. The spectrum of the fluctuations is well fit by a CBR spectrum. When coadded in CBR temperature units, the RMS of the observed structure is 145 μK, or $\Delta T/T = 5.3 \times 10^5$. Following is a brief discussion of possible origins of the structure other than CBR fluctuations.

Sidelobe contamination is considered an unlikely source of the structure. The best evidence for this is the Mu Pegasi data set discussed above. Those data were taken while the telescope tracked from 36°to55° in elevation. Sidelobe contamination from the ground should be greater in the first half of the Mu Pegasi measurement than in the GUM measurement, while contamination from the balloon emission would be greater in the second half of the Mu Pegasi measurement than in the GUM measurement. The 95% confidence level upper limits to

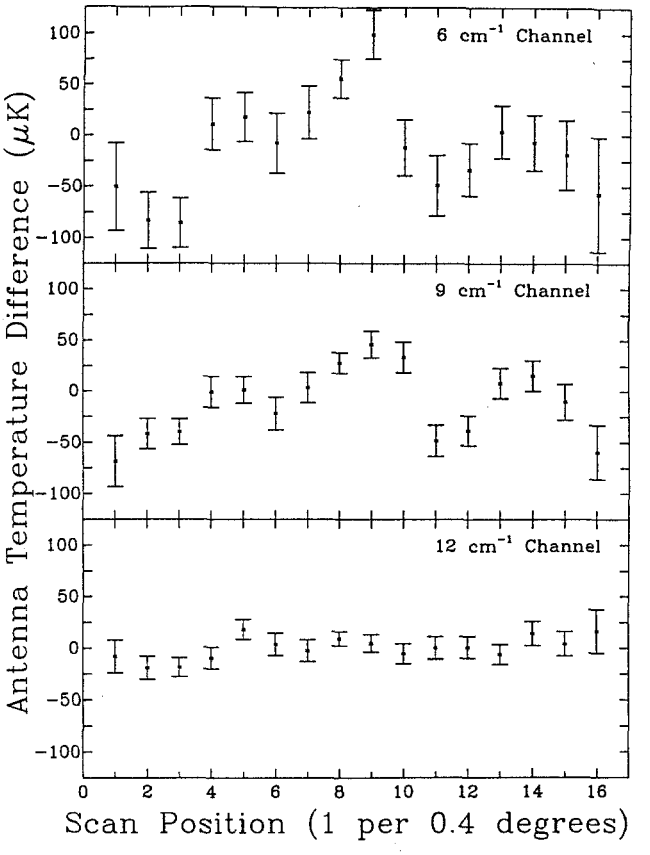

Fig. 7. 16 of 39 points from MAX III GUM data set. Vertical axis is again in antenna temperature units. Scaling to thermodynamic units is the same as Figure 6.

GACF CBR fluctuations for the Mu Pegasi data set first and second halves are 71 μK and 79 μK respectively, well below the measured signal.

The spectrum of the measured signal is extremely different from ISD. In addition, an extrapolation of the IRAS 100 μ data for GUM using the Mu Pegasi dust data predict very low differential dust emission.

Galactic synchrotron emission can be conservatively estimated by scaling the Haslam et al (1982) map, assuming antenna temperature scales as $\nu^{-2.7}$. This estimate provides less than 1% of the measured signal. Free-free emission is more difficult to estimate, but a similar conservative approach of assuming all signal in the Haslam map is due to free-free emission and scaling by $\nu^{-2.1}$ produces only 10% of the measured signal (and no significant morphological correlation).

Measurements of the CO(J=1-0) transition in this region (Wilson and Koch 1992, Thaddeus and Dame 1993) show there is no emission above 1 K km s^1. A 1 K km s^1 CO cloud filling a beam would give approximately a 10 μK signal at 6 cm^{-1} and a 5-10 μK signal at 9 cm^{-1}.

Figure 8 shows the weighted average of the 6 and 9 cm^{-1} data for the same set of points as Figure 7, rescaled to CBR thermodynamic temperature units. Under the assumption that the signal measured in the GUM region is due to CBR fluctuations, both upper and lower limits have been calculated for GACF at 25 arcminutes. At 95 % confidence level, the lower limit is $\Delta T/T > 3.1 \times 10^{-5}$, the most probable amplitude is $\Delta T/T = 4.2 \times 10^{-5}$ and the upper limit is $\Delta T/T < 5.9 \times 10^{-5}$.

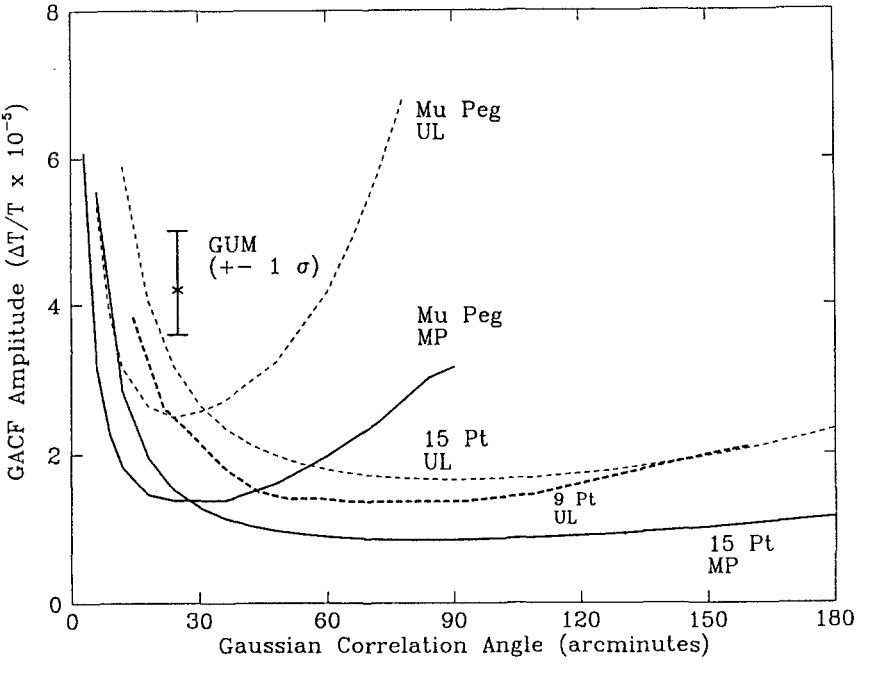

Fig. 8. 16 of 39 points from MAX III GUM data set, weighted average of 6 and 9 cm^{-1} channels. Vertical axis is in thermodynamic temperature units relative to a 2.73 K blackbody.

5 Comparisons and Discussion

Figure 9 shows all four data sets analyzed in the same way (using a GACF model). As noted earlier, the GACF is used primarily to allow a direct comparison among results at similar angular scales without reference to a cosmological model. It should be kept in mind that the upper limit curves are formally valid over the entire range, and exclude GACF skies with amplitudes larger than the curve at every point, at the 95% level. The detection or "most probable" curves are *not* valid over the entire range, but only pointwise. The best way to compare data sets is to compare the lowest point on the most probable curve to the same

angular scale point on the upper limit curve. The most striking feature of the four data sets, aside from their sensitivity, is the apparent conflict between the two MAX 3 measurements, under the assumption of Gaussian distributed fluctuations described by a GACF. In fact, the upper limits from Gaier et al (1992) and Schuster et al (1993) are both also in apparent conflict with the GUM result. If the GUM data are correct, and are describing fluctuations in the CBR, then either our assumptions about the distribution of fluctuations are in question, or the sampling performed thus far in medium scale CBR anisotropy searches is inadequate. Note that we have only sampled less than 1% of the celestial sphere, with the combined data from both experiments.

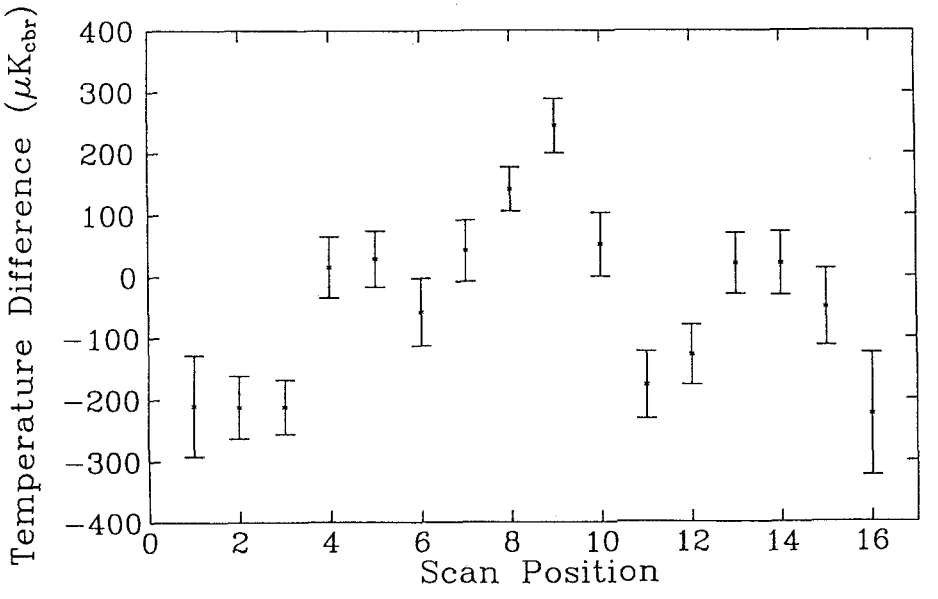

Fig. 9. Upper limits (UL) and most probable (MP) signals calculated from the data of Gaier et al (1992) (9 Pt), Schuster et al (1993)(15 Pt), Meinhold et al (1993) (Mu Peg) and Gundersen et al (1993)(GUM). The single point with error bars is the GUM detection, with $\pm 1\sigma$ errors. Dotted lines indicate 95% confidence level upper limits, solid lines indicate most probable signal levels (under the assumption that all relevant structure is due to CBR fluctuations).

The current generation of degree scale CBR anisotropy experiments has been forced to concentrate on extremely small areas of the sky, by a combination of foreground emission, available integration time (or detector sensitivity), and the need to control sources of systematic error extremely well. Currently planned array systems should help to alleviate the integration time and systematic error control problems at least.

6 Current Work

6.1 MAX 4

The MAX experiment flew in June, 1993 for the fourth time. In its latest incarnation, the detector was upgraded to an ADR, which kept the bolometers at a temperature of 85 mK, increasing the sensitivity. A fourth frequency channel was added near 90 GHz, to aid in discrimination of CBR from free-free emission. Three deep CBR integrations were performed, including one on the GUM region. Analysis of the data is proceeding.

This system is expected to fly again in May or June of 1994. Several more CBR anisotropy targets will be measured, as well as an attempt to measure the Sunyaev-Zeldovich effect towards Coma.

6.2 South Pole HEMT work

A new set of experiments is currently en route to the South Pole for an Austral summer season of observing. Two 1 meter Gregorian telescopes and a prime focus system will make observations with FWHM ranging from 1° to 4°. Multi-frequency HEMT detectors similar to the one described above, but operating from 38-45 GHz and 26-36 GHz will be used on the telescopes.

6.3 Acknowledgements

The data reported here are the results of the concerted efforts of a large number of people over several years. Current contributors to the MAX effort include Andre Clapp, Mark Devlin, Marc Fischer, Andrew Lange, Paul Richards, and Stacy Tanaka of the Physics department of the University of California at Berkeley and Joshua Gundersen, Mark Lim, Philip Lubin, and P. Meinhold of the University of California at Santa Barbara.

The ACME-HEMT results are the work of Todd Gaier, Joshua Gundersen, Timothy Koch, Michael Seiffert, Jeffrey Schuster, Alexandre Wuenche, Philip Lubin and P. Meinhold, of the University of California at Santa Barbara.

All of those named above are also members of the NSF Center for Particle Astrophysics (CfPA).

This work has been supported by NASA under grant NAGW-1063; the NSF, under Polar grant NSF DPP 89-20578; and the Center for Particle Astrophysics. We wish to thank the entire ASA staff at the South Pole station for their excellent support during the 1990-91 season. We would also like to thank the NSBF crews for all the great flights, particularly June, 1991, and June, 1993. The K_a band HEMT amplifiers are on loan from the NRAO CDL. We are gratefull to Mike Balister, Marian Pospieszalski, and the staff of the NRAO CDL for their patience during numerous conversations on the subject of low noise amplification.

References

Alsop, D. C.,Cheng, E. S., Clapp, A. C., Cottingham, D. A., Fischer, M. L., Gundersen, J. O., Koch, T. C., Kreysa, E., Meinhold, P. R., Lange, A. E., Lubin, P. M., Richards, P. L., and Smoot, G. F. Astrophys. J. **317** (1992) 146

Devlin, M., Alsop, D., Clapp, A., Cottingham, D., Fischer, M., Gundersen, J., Holmes, W., Lange, A., Lubin, P., Meinhold, P., Richards, P., Smoot, G., 1992; Proc. Nat. Acad. Sci. USA (1992)

Fischer, M. L., Alsop, D. C.,Cheng, E. S., Clapp, A. C., Cottingham, D. A., Gundersen, J. O., Koch, T. C., Kreysa, E., Meinhold, P. R., Lange, A. E., Lubin, P. M., Richards, P. L., and Smoot, G. F. Astrophys. J. **388** (1992) 242

Gaier, T., Schuster, J. A., Gundersen, J. O., Koch, T., Seiffert, M. D., Meinhold, P. R., Lubin, P. M. Astrophys. J. **398** (1992) L1

Gundersen, J. O., Clapp, A.C., Devlin, M., Holmes, W., Fischer, M. L., Meinhold, P. R., Lange, A. E., Lubin, P. M., Richards, P. L., and Smoot, G. F.**413** L1-L5

Meinhold, P. R., and Lubin, P. M. Astrophys. J. **370** (1991) 11

Meinhold, P., Clapp, A., Devlin, M., Fischer, M., Gundersen, J., Holmes, W., Lange, A., Lubin, P., Richards, P., and Smoot, G. Astrophys. J. **409** (1993) L1

Meinhold, P. R., Chingcuanco, A. O., Gundersen, J. O., Schuster, J. A., Seiffert, M. D., Lubin, P. M., Morris, D., and Villela, T. Astrophys. J. **406** (1993) 12

Pospieszalski, M. W., Gallego, J. D., Lakatosh, W. J. Proc. 1990 MTT-S Int. Microwave Symp. (1990) 1253.

Schuster, J., Gaier, T., Gundersen, J., Meinhold, P., Koch, T., Seiffert, M., Wuensche, C., and Lubin, P. Astrophys. J. **412** (1993) L47